JOURNAL OF ENVIRONMENTAL SCIENCES 53 (2017) 184–195

Available online at www.sciencedirect.com

ScienceDirect

www.elsevier.com/locate/jes

JES JOURNAL OF ENVIRONMENTAL SCIENCES

www.jesc.ac.cn

Online single particle measurement of fireworks pollution during Chinese New Year in Nanning

Jingyan Li[1], *Tingting Xu*[1], *Xiaohui Lu*[1], *Hong Chen*[1], *Sergey A. Nizkorodov*[2], *Jianmin Chen*[1,3], *Xin Yang*[1,3,*], *Zhaoyu Mo*[4], *Zhiming Chen*[4], *Huilin Liu*[4], *Jingying Mao*[4], *Guiyun Liang*[4]

1. *Shanghai Key Laboratory of Atmospheric Particle Pollution and Prevention, Department of Environmental Science and Engineering, Fudan University, Shanghai 200433, China. E-mail: jingyanli12@fudan.edu.cn*
2. *Department of Chemistry, University of California, Irvine, California 92697, United States*
3. *Fudan-Tyndall Center, Fudan University, Shanghai 200433, China*
4. *Guangxi Academy of Environmental Sciences, Nanning 530022, China*

ARTICLE INFO

Article history:
Received 17 January 2016
Revised 17 April 2016
Accepted 19 April 2016
Available online 3 June 2016

Keywords:
Chinese New Year
Fireworks
Particle types
Secondary process

ABSTRACT

Time-resolved single-particle measurements were conducted during Chinese New Year in Nanning, China. Firework displays resulted in a burst of SO_2, coarse mode, and accumulation mode (100–500 nm) particles. Through single particle mass spectrometry analysis, five different types of particles (fireworks-metal, ash, dust, organic carbon-sulfate (OC-sulfate), biomass burning) with different size distributions were identified as primary emissions from firework displays. The fireworks-related particles accounted for more than 70% of the total analyzed particles during severe firework detonations. The formation of secondary particulate sulfate and nitrate during firework events was investigated on single particle level. An increase of sulfite peak ($80SO_3^-$) followed by an increase of sulfate peaks ($97HSO_4^-$+$96SO_4^-$) in the mass spectra during firework displays indicated the aqueous uptake and oxidation of SO_2 on particles. High concentration of gaseous SO_2, high relative humidity and high particle loading likely promoted SO_2 oxidation. Secondary nitrate formed through gas-phase oxidation of NO_2 to nitric acid, followed by the condensation into particles as ammonium nitrate. This study shows that under worm, humid conditions, both primary and secondary aerosols contribute to the particulate air pollution during firework displays.

Introduction

Fireworks or crackers, which are commonly set off during celebrations and vacations, are unique anthropogenic sources that generate massive quantities of air pollutants within a short span of time. In general, fireworks consist of three main components: oxidants, flammable materials and flame agents. Potassium compounds in the form of nitrates, perchlorates, and chlorate (much less common) usually act as main oxidizers in commercial fireworks. Charcoal and sulfur are burnt as fuel when setting off fireworks. Elements, metal chlorides, metal nitrates or metal carbonates are usually added to produce different flame colors. Burning of fireworks can release great amount of gaseous pollutants (SO_2, NOx, CO, *etc.*) and suspended particles in short span of time (Barman et al., 2008; Beig et al., 2013). In general, the aerosols emitted by fireworks are composed of metals (e.g., K, Mg, Sr, Ba, Cu, Mg and Al), elemental carbon, organic carbon and inorganic anions such as SO_4^{2-}, Cl^- and NO_3^- in both coarse and fine mode (Moreno et al., 2007; Croteau et al., 2010; Sarkar

* *Corresponding author*. E-mail: yangxin@fudan.edu.cn (Xin Yang).

http://dx.doi.org/10.1016/j.jes.2016.04.021
1001-0742/

et al., 2010; Zhang et al., 2010; Crespo et al., 2012; Do et al., 2012). Firework displays are associated with serious health hazards (Lemieux et al., 2004; Shi et al., 2011), ecological impacts (Sijimol and Mohan, 2014) and may result in serious accidents and lethal injuries (Puri et al., 2009).

Chinese New Year (CNY), which is also called Spring Festival, is an important Chinese festival celebrated with intensive firework displays all over the China both in megacities and in rural areas. CNY celebrations traditionally start from Chinese New Year's Eve (NYE) and last for 7 or 15 days. Chinese government reported that more than 1500 tons of fireworks debris could be generated during a NYE in a middle scale city. Although fireworks activities usually take a relatively short time, the high concentrations of gaseous and particulate pollutants can have huge impacts on air quality (Yerramsetti et al., 2013). Due to the formation of atmospheric inversion in winter season, pollutants may be trapped close to ground level, resulting in long-term haze and visibility reduction. As firework displays generate massive amounts of particulate matter precursors such as SO_2, NOx, and organic compounds, secondary processes between gas-phase and particle-phase compounds may lead to production of secondary air pollutants after firework displays. Since other forms of anthropogenic emissions usually decrease during holidays, CNY also provides scientists with an opportunity to study short-term degradation of air quality and its possible human health impacts under reduced emission conditions.

Previous research on CNY events examined total particle mass, composition and aging processes based on conventional filter measurements, which provide average properties of particles. Morphology and chemical composition of individual long-range transported fireworks aerosols and lab-generated samples were investigated by transmission electron microscopy, revealing that firework emissions during the CNY significantly changed the atmospheric transformation pathway of SO_2 to sulfate (Li et al., 2013). However, information on the properties of individual fireworks aerosol particles is still limited.

Furthermore, CNY firework event is a short-time air pollution episode, and the off-line methods may not have enough time resolution to capture its chemical evolution. In order to establish a better understanding on the rapid formation and composition evolution of firework displays, time-resolved measurements are required. Only a few real-time measurements of particle composition were conducted during CNY events. An aerosol chemical speciation monitor (ACSM) was used to achieve the first real-time measurements during a CNY event, however the information on metal constituents of particles was not acquired due to the limitations of the ACSM instrument (Jiang et al., 2015). Aerosol time-of-flight mass spectrometer (ATOFMS) has been proven to successfully detect heavy metals emitted from firework displays (Liu et al., 1997). Positive matrix factorization was applied to identify firework-family particles detected by ATOFMS in U.S. (McGuire et al., 2011). Previous single-particle mass spectrometry measurements mainly aimed at distinguishing unique firework particles, especially those containing metals, from particles found in the ambient environment. However, different types of particles could be co-emitted from a single source. In this study, we focus both on the identification of different types of particles emitted by fireworks and on the real-time analysis of the chemical processes that occurred on particles after the firework displays.

Several field measurements based on filter samples collected during CNY events have been reported in Beijing (Wang et al., 2007; Huang et al., 2012), Jinan (Li et al., 2013; Yang et al., 2014), Tianjin (Tian et al., 2014), Shanghai (Zhang et al., 2010; Feng et al., 2012), Nanjing (Kong et al., 2014) and Lanzhou (Shi et al., 2011; Zhao et al., 2014). It is the first time to investigate firework displays in Nanning, which is quite different in terms of environmental conditions from the previously examined sites. Specifically, the higher temperature and relative humidity in Nanning might favor secondary chemical processes that are unique to this geographic location.

1. Experiment and methods

1.1. Ambient individual particle observation by SPAMS

The design and operation of the single particle aerosol mass spectrometer (SPAMS, Hexin Analytical Instrument Co., China) used in this study is described in detail elsewhere (Li et al., 2011). In brief, after passing through a 0.1 mm orifice at a flow of 0.08 L/min, the air is drawn into a series of aerodynamic lens of SPAMS, where the particles are focused and accelerated to their terminal velocity. The particles then pass through two continuous neodymium-doped yttrium aluminum garnet (Nd:YAG) laser beams (532 nm). The time difference between the two scattering signals is used to calculate the velocity and vacuum aerodynamic diameter (D_{va}) of individual particles. The scattering signals also trigger the firing of a Nd:YAG laser (266 nm), operating at 0.5 mJ, for the desorption and ionization of each sized particle. Dual polarity time-of-flight mass spectra are acquired after each laser pulse. Polystyrene latex spheres (PSL, 0.2–2.0 μm) and standard metal solutions were used to calibrate particle size and mass before sampling. In general, the SPAMS instrument used in this work shares the similar aerosol sampling methods, sizing and desorption/ionization modules as better known ATOFMS (Li et al., 2014), and it has been proven to achieve comparable single-particle sensitivity and time resolution.

A total of approximately 350,000 particles, with both positive and negative ion spectra, were analyzed (34% of total sized particle). Particles' sizes and individual mass spectra were imported into MATLAB and further analyzed with YAADA (Yet Another ATOFMS Data Analyzer, www.yaada.org), a software toolkit for processing single-particle mass spectra. Individual particle clustering was performed with Art-2a (adaptive resonance theory based neural network algorithm) (Song et al., 1999), based on the presence and intensities of ion peaks in individual mass spectra. The parameters applied in the algorithm were set as: vigilance factor: 0.85; learning rate: 0.05; and number of iterations: 20. Nearly 5000 particle clusters were gained and then re-grouped again using the same Art-2a parameters to reduce the number of particle types. The resulting particle clusters were further manually merged into 14 particle sub-types, and then grouped to 7 main groups, based on the similar mass pattern, time variation and size distribution. All the grouped particles accounted for ~95% of all analyzed particles, implying the result can be representative

of overall sampled particles. No significant temporal trend was found for the unclassified particles.

1.2. Sampling site and period

Nanning is a city located in southwestern China (Fig. S1a). Ambient measurements by SPAMS, Scanning Mobility Particle Sizer (SMPS), Aerosol Particle Sizer (APS), were conducted at the Nanning Environmental Science Research Institute Super Site (22°48′N, 108°20′E). The sampling site is surrounded by heavy traffic, restaurants, and residential areas, so it is representative of Nanning urban area. All the instruments were set up on the roof of a five-story building (~20 m high). Aerosols were drawn through a $PM_{2.5}$ cyclone at a flow rate of 3 L/min before entering the instruments in order to remove coarse particles. Particle mobility-equivalent diameter (D_m) distributions were measured from 14.1 to 710.5 nm using a TSI scanning mobility particle sizer (SMPS3081, TSI, USA). Time variation of particle numbers with a size range from 0.5 to 20 μm was measured by a TSI aerosol particle sizer (APS3321, TSI, USA). SMPS and APS provided data every 5 min synchronously. The metrological data (temperature, relative humidity, wind speed and wind direction), hourly averaged mass concentration of particulate matter ($PM_{2.5}$ and PM_{10}) and gaseous pollutants (SO_2, NOx (NO + NO_2), O_3 and CO) were measured at the nearest Nanning City Monitoring Station (22°49′N 108°19′E, ~2 km away). Usually, fireworks were set off by citizens along residential avenues all over the city. Thus, it can be assumed that the two measurement sites were experienced similar levels of firework-related emissions.

Field measurements of CNY in Nanning lasted approximately 6 days, from 30-Jan-2014 12:00 to 5-Feb-2014 00:00, covering tradition holidays of the Chinese Spring Festival. Usually, fireworks and crackers are set off to celebrate holiday in the evening hours. The most intensive firework displays happen on Chinese New Year's Eve (NYE), lasting from the evening to the early following morning. In addition, a large amount of firework displays and crackers are also set off to welcome the God of Wealth (GOW) from the fourth day afternoon till the midnight of the fifth day of the Lunar Calendar. Based on this fact, the air quality around the midnight of 31-Jan-2014 (NYE) and 4-Feb-2014 (GOW) might be influenced by fireworks/crackers detonation greater than other episodes.

2. Result and discussion

2.1. Time variation of mass concentration, number concentration of particulate matter

Fig. 1 depicts hourly variations of metrological parameters (temperature, relative humidity, wind speed, wind direction), mass concentrations of particles (PM_{10}, $PM_{2.5}$) and gas pollutants (SO_2, CO, NOx, O_3) during sampling period. A clear diurnal variation of temperature and RH can be seen in the figure. The average values of temperature and RH were (19.1 ± 3.5)°C and (70 ± 15)%, and the wind speed kept at relatively low value (<4 m/sec), giving a mild and humid weather condition. $PM_{2.5}$ and PM_{10} concentrations in Nanning varied over a large range during the measurement period. Heavy PM pollution, together with high mass concentration of SO_2, occurred on NYE when the firecrackers were extensively used. PM_{10} and $PM_{2.5}$ increased by a factor of 10 and 4 within 2 hr with peak values of 1.73 and 0.399 mg/cm^3, respectively, suggesting that firework displays had strong impacts on both coarse and fine particle pollution. Compared with previous observations (Huang et al., 2012; Tsai et al., 2012), PM_{10} pollution was more severe in Nanning during CNY, which might be causes by less government regulation and more cracker detonations. SO_2 concentration also reached a large value of 0.521 mg/m^3, as fireworks/crackers contains high amount of sulfur, which burns in air producing SO_2. With decreasing frequency of firework displays, gaseous and particulate pollutants mass concentrations dropped slightly. The relatively low wind speed (1 m/sec) and weak vertical mixing during night time (Fig. S1b) hindered the diffusion of pollutants, so the high pollution levels lasted for nearly 12 hr during NYE. Another increase of mass concentration of PM and SO_2, accompanied by an increase in the levels of CO and NOx also occurred around GOW. Other periods (for example, 1-Feb-2014 and 2-Feb-2014) were relatively clean with average $PM_{2.5}$ value of (0.046 ± 0.013) mg/m^3 and no distinct peaks of particle loading, SO_2, NOx and CO, indicating light firework influences.

Fig. 2a illustrates the temporal variations of particle number concentrations detected by SPAMS and APS during the sampling period. The peaks of particle number concentration happened around 31-Jan-2014 00:00, 31-Jan-2014 10:00 and 4-Feb-2014 00:00, at the same time when PM_{10} and $PM_{2.5}$ increased. The sampling ranges of APS and SPAMS were quite similar with using $PM_{2.5}$ cyclone, and fair correlation between particle number concentrations was observed (r = 0.73). As shown in Fig. 2b, the detonation of fireworks had a clear contribution to the number concentration of accumulation mode particles (100–500 nm) on NYE, similar to the results reported in previous studies (Zhang et al., 2010; Dutschke et al., 2011; Zhao et al., 2014). The mode diameter of particles detected by SMPS also increased nearly twice within two hours. A substantial increase of particle mean diameter from 100 to 150 nm was observed on GOW, likely resulting from secondary processes happening under stagnant condition (Guo et al., 2014). Therefore, GOW might not be a typical fireworks pollution episode in our case.

2.2. Particle classification

Classified particles with dual mass spectrum detected by SPAMS were analyzed to better understand the influence of fireworks displays. Generally, the positive mass spectra are analyzed to distinguish main sources (Dall'Osto and Harrison, 2006; Wang et al., 2014), while the negative mass spectra provide more information about aging processes. Therefore, both positive and negative mass spectra were used to classify particles in this study.

Table 1 shows the names, numbers and number fractions of individual groups and sub-types. Five sub-types (organic carbon-sulfate (OC-sulfate), dust, ash, fireworks-metal, biomass burning) marked with bold style were identified as fireworks-related clusters according to their characteristic peaks and

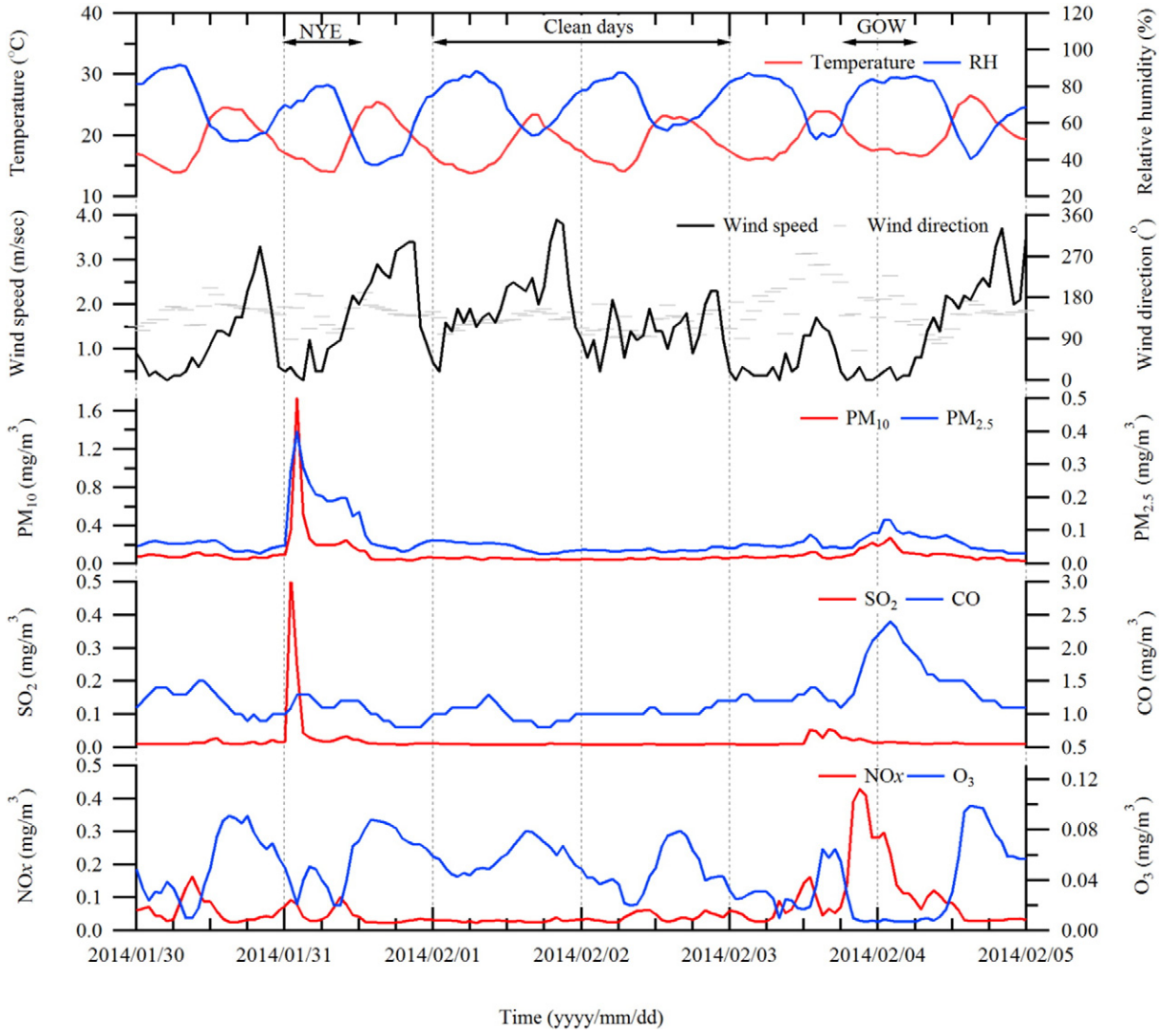

Fig. 1 – Hourly variation of metrological parameters (temperature, relative humidity, wind speed, wind direction), particle loading (PM_{10}, $PM_{2.5}$) and concentrations of gas pollutants (SO_2, CO, NOx, O_3). NYE: New Year's Eve; GOW: God of Wealth.

similar time dependence. The detailed mass spectral features of all particles can be found in supplementary information section. Clusters of firework-related particles are discussed in the next paragraphs. The corresponding average mass spectral patterns are illustrated in Fig. 3 and Fig. S2.

2.2.1. *Fireworks-metal*

Single particles contained strontium ($88Sr^+$), barium ($138Ba^+$, $154BaO^+$) had been distinguished as fireworks particles by ATOFMS (Liu et al., 1997; McGuire et al., 2011). In our research, more species of metals of lead ($206/207/208Pb^+$), copper ($63/65Cu^+$) and aluminum ($27Al^+$) were found to be released as fireworks-metal particles, which were in consistence with off-line observations (Camilleri and Vella, 2010; Crespo et al., 2012).

Ash are potassium-rich particles intermixed with chlorine ($39K^+$, $35/37Cl^-$, $113/115K_2Cl^+$, $109/111KCl_2^-$), nitrate ($46NO_2^-$, $62NO_3^-$) and sulfate ($48SO^-$, $64SO_2^-$, $80SO_3^-$, $96SO_4^-$). Particles containing potassium chloride and potassium nitrate fragments ($140K_2NO^+$, $147KNO_3NO^-$, $163K(NO_3)^-$) were identified as fireworks family by ATOFMS before (Jeong et al., 2011; McGuire et al., 2011). In our case, only 7.13% of ash particles contained potassium nitrate fragments. One possible reason is that previous studies sampled aged polluted plumes, which were transported from emission sources several miles away from the sampling site, so heterogeneous reaction $HNO_3 + Cl^- \rightarrow NO_3^- + HCl$ might happen on fireworks particles, increasing the observed fraction of nitrate ions. The observation of chemical processing of firework produced particles during long-rang transported exhibited the exchange between Cl^- and other secondary species (Li et al., 2013), which verified our assumption somehow.

Dust particles contain two subtypes: MgAlSi and CaSi, which were either related to black powder components or crustal elements. Soil dusts are usually added during manufacturing fireworks/crackers to prevent accidental explosion. Also, severe explosion of fireworks could lead to the re-suspension of road dust (Tian et al., 2014). It should be noted that dust particles observed in this work had a strong peak of chlorine ($35/37Cl^-$),

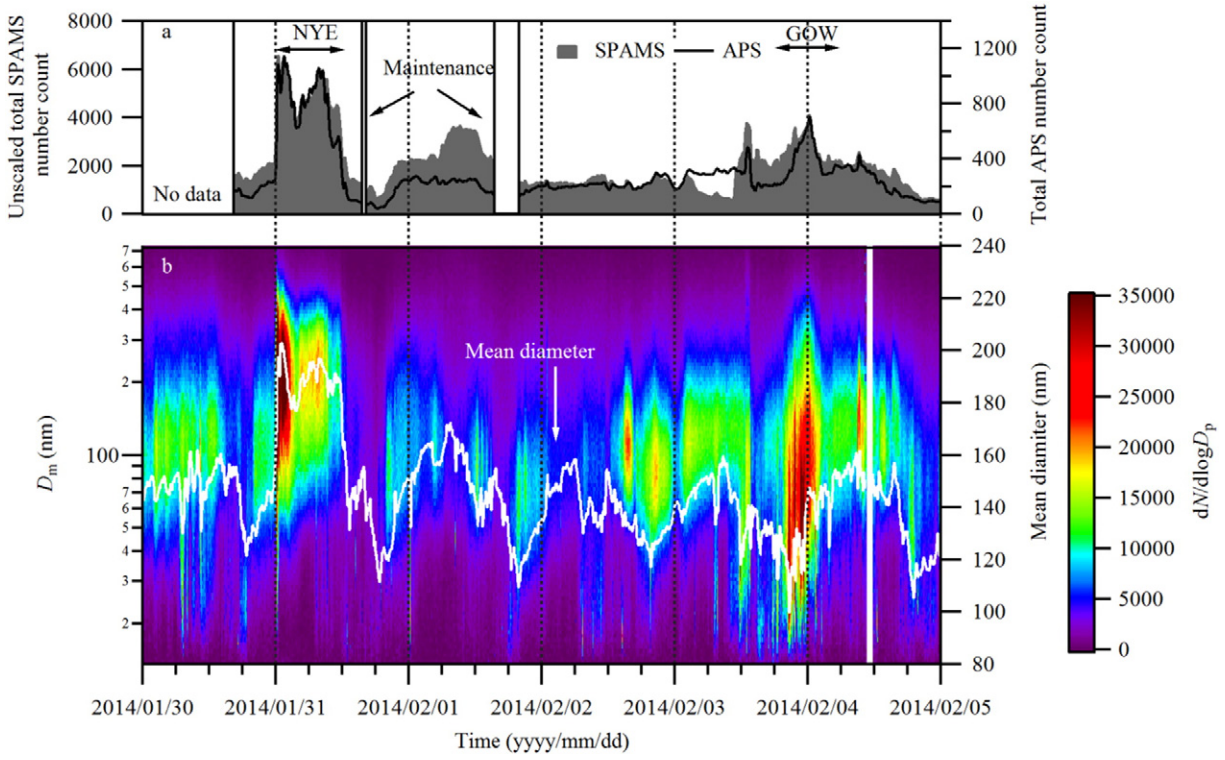

Fig. 2 – (a) Time variation of unscaled particle number counts detected by laser-sizing in single particle aerosol mass spectrometer (SPAMS) (vacuum aerodynamic diameter 0.2–2 μm) and particle number concentration detected by Aerosol Particle Sizer (APS) (aerodynamic diameter 0.542–20 μm); (b) Size distribution and mean diameters of particles measured by Scanning Mobility Particle Sizer (SMPS) in the mobility diameter (D_m) range of 14.1–700 nm.

providing evidence that most of dust particles observed in our case were mixed with black power compounds and could be emit from firework displays.

Table 1 – Names, numbers and fractions of the 7 main particle types (14 sub-types) identified by single particle aerosol mass spectrometer.

Group	Number	Fraction	Cluster	Fraction
OC	54,912	15.59%	**OC-sulfate**[a]	8.19%
			OC-nitrate	4.81%
			HMOC	2.58%
EC	76,954	21.85%	EC/KEC/NegEC	21.85%
ECOC	2556	0.73%	ECOC	0.73%
Dust	3223	0.91%	**MgAlSi/CaSi**	0.91%
Sea salt	2199	0.62%	Sea salt	0.62%
Ash/metal	10,287	2.92%	**Ash**	1.27%
			Fireworks-metal	1.06%
			Industrial-metal	0.59%
K-rich	184,078	52.26%	K-ECOC-sulfate	14.26%
			K-ECOC-nitrate	13.13%
			K-secondary	12.70%
			Biomass burning	12.17%
Others	18,050	5.12%	Unclassified	5.12%
Sum	352,259	100.00%		100.00%

OC: organic carbon; HMOC: high mass organic carbon; EC: elementary carbon.
[a] The names in bold style are likely contributed by the burning of fireworks/crackers based on their time variations.

OC-sulfate counts increased strikingly on the midnight of NYE and had a good correlation with $PM_{2.5}$ temporal variation (r = 0.88) and raw SPAMS count (r = 0.78), relating to firework displays more closely than other organic clusters. Previous studies demonstrated that firework displays had clear contributions to organic carbon (OC) (Drewnick et al., 2006; Feng et al., 2012), but the types of organic compounds were not well-known. Nishanth and coworkers discovered aliphatic compounds in particle phase during firework displays (Nishanth et al., 2012). Jiang and coworkers indicated that OC emitted from CNY were mainly dominated by low volatility secondary organic aerosol (Jiang et al., 2015). Volatile organic carbon was found to elevate during CNY in Nanjing (Kong et al., 2015a, 2015b). Previous studies disagreed on whether firework displays were large sources for polycyclic aromatic hydrocarbon (PAH) (Sarkar et al., 2010; Feng et al., 2012; Kong et al., 2015a, 2015b). In our observations, the peak of OC-sulfate counts appeared together with particle pollution on NYE with a sudden decrease of oxidized marker ratio ($43C_2H_3O^+/27C_2H_3^+$), indicating that firework displays were the primary sources of OC. Peaks of $63C_5H_3^+$ and $77C_6H_5^+$ can be observed on mass spectrum, which were fragments of aromatic compounds (Silva and Prather, 2000). In our observation, OC-sulfate cluster only had fair correlation (r = 0.56) with high mass organic carbon (HMOC) (including PAH), indicating that firework displays emitted less PAH compounds. The elevated organic compound during firework display might be produced from volatile phenyl compounds

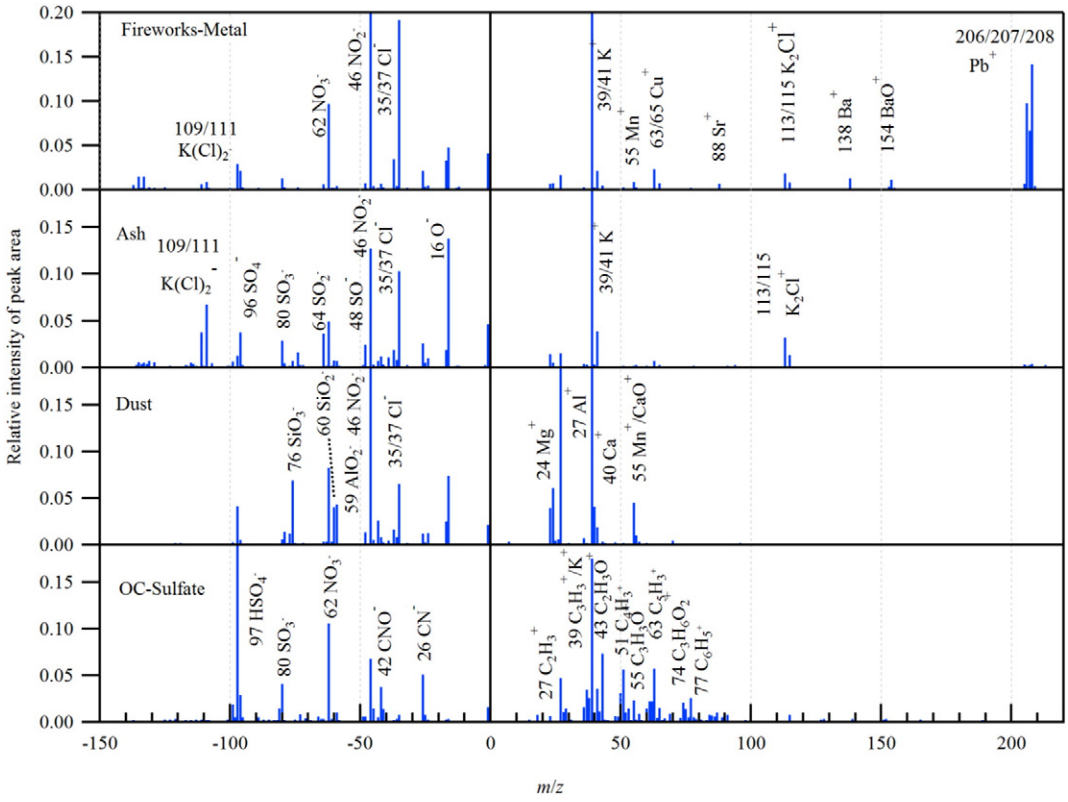

Fig. 3 – Average mass spectra of firework-related clusters (fireworks-metal, ash, dust and OC-sulfate). Characteristic ion peaks used for the identification of different clusters are marked with possible atomic composition.

used as adhesive materials in fireworks or crackers. Besides, the burning of charcoal and paper package might also be responsible for the elevated concentration of the OC.

2.2.2. Biomass burning

The number count and fraction of biomass burning particles exhibited peaks around 31-Jan-2014 00:00 and 4-Feb-2014 00:00 and shared good correlation with OC-sulfate (r = 0.88), indicating firework display were direct sources. Fireworks or crackers are packed with paper rolls, biomass combustion could be caused by both directly firework explosions and burning of fireworks debris. It should be noted that biomass burning particles can have other sources, such as biofuel burning. In our case, the we include them in the fireworks-related clusters because previous observations found that they could contributed to around 15% of PM generated by firework pollutions (Tian et al., 2014).

Fig. 4 shows the size resolved number fractions of classified particle types in size range from 0.2 to 2.0 μm (D_{va}) during the entire sampling period. It should be stressed that the size distributions presented in this work have only semi-quantitative meaning, as the SPAMS efficiency varies with different particle species. Fireworks-related clusters showed two different size distributions. OC-sulfate and biomass burning clusters contained mainly submicron particles (0.4–1 μm). Fireworks-metal, ash, and dust clusters mostly distributed in coarse mode (1.0–2.0 μm), with a median value of 1.08 μm, 1.15 μm, and 1.12 μm, respectively. The observed particle sizes are somewhat larger than the previous results observed by ATOFMS (McGuire et al., 2011), due to the close vicinity to firework display spots and more detonations of crackers. The firework display markers identified by the previous studies were mostly ash, dust and fireworks-metal particles in the coarse mode. Our study demonstrates that firework displays were also important sources of submicron particles including OC-sulfate and biomass burning particles in Nanning.

2.3. Temporal variations of different particle types

Fig. 5 shows temporal variations of SPAMS-identified cluster counts and number fractions with 15-min time resolution. Before NYE, the number of particles sized by SPAMS was relatively low. The most abundant particles were potassium-elementary carbon and organic carbon-sulfate (K-ECOC-sulfate) and elementary carbon (EC), making up nearly 60% of total particles, which were mainly from stationary source emissions and vehicle exhaust. When intense firework displays happened, the fractions of fireworks-related clusters: fireworks-metal, ash, dust, OC-sulfate and biomass burning sharply increased and reached a maximum over 70% of total particles around the midnight of NYE. Liu et al. (1997) reported that pyrotechnically derived particles, which correspond to Fireworks-metal and ash particles in our research, accounted for almost 20% of ATOFMS-detected particles. Our result is higher since OC-sulfate and biomass burning particles are also

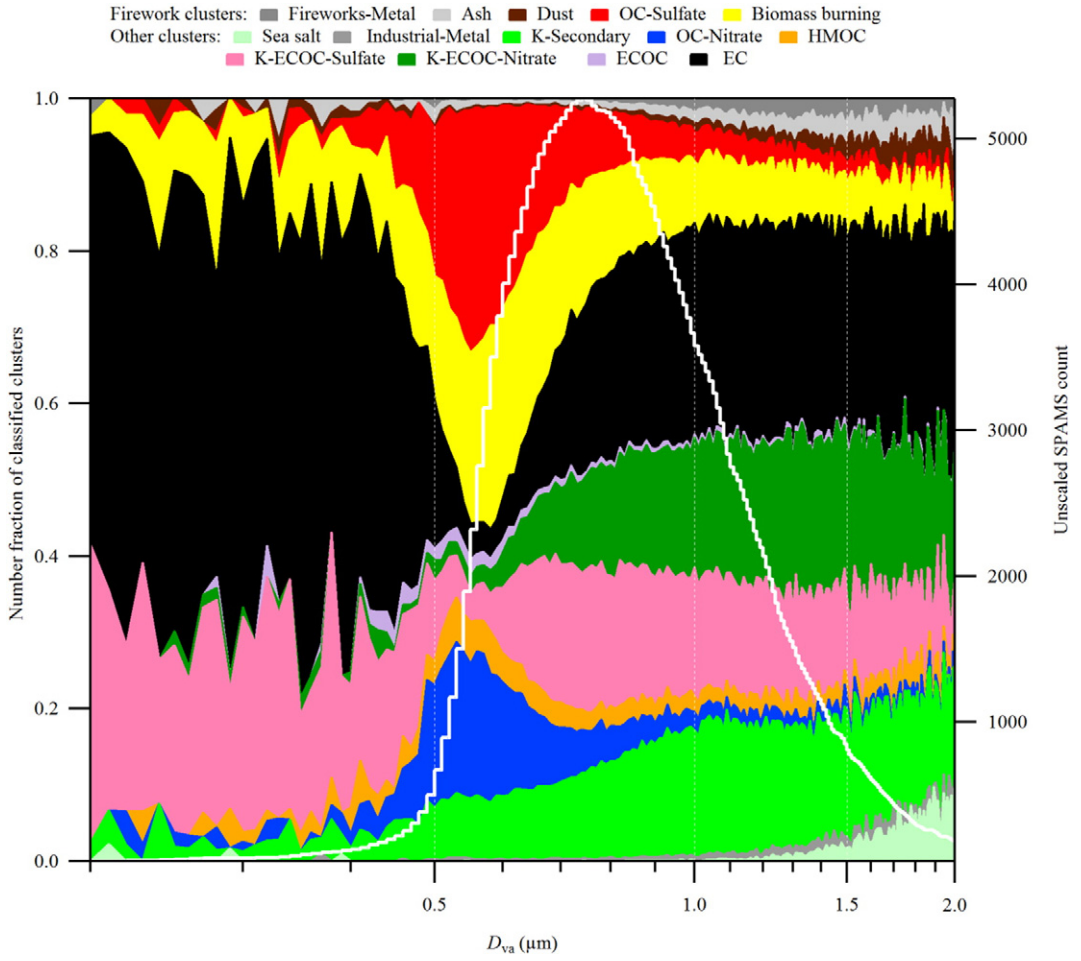

Fig. 4 – Chemically resolved size distributions of cluster number fractions (color-coded shading) and the size distribution of unscaled single particle aerosol mass spectrometer (SPAMS)-analyzed particle number counts (white line).

included in the fireworks-related clusters. Thereafter, both the raw SPAMS particle counts and the number fraction of fireworks-related particles decreased gradually. Meanwhile, a slight increase of the K-secondary cluster from 8.7% to 20.8% was observed. Atmospheric aging processes probably modified the chemical composition of firework-related particles and enhanced secondary particle fraction under stagnant condition. After NYE, the number fraction of fireworks-related clusters gradually returned to the before-NYE level. At the same time, the fraction of sea-salt particles increased to 5.0%, indicating that the clean air masses transported from sea helped dilute firework pollutions.

Similar to NYE, the fraction of fireworks-related clusters also increased during GOW and accounted for 50% of SPAMS-detected particles at the peak because additional firework/cracker detonation took place. Compared with NYE, the fraction of K-ECOC-nitrate, OC-nitrate and HMOC increased in GOW, which were attributed to aged urban particles in the supplementary information section. Compared to the NYE period, the average mass spectrum observed during the GOW celebrations also exhibited more markers of nitrate and oxidized carbon ($89CH_3COOH^-$, $43C_2H_3O^-$). Therefore, particles detected during the GOW celebrations contained more aged compounds, indicating particle accumulation and aging effect was another important cause for the pollution.

The period between NYE and GOW was relatively clean (1-Feb-2014 00:00–3-Feb-2014 00:00) with low total particle counts. The most abundant clusters were EC, K-ECOC-sulfate and K-ECOC-nitrate. The high fraction of EC particles can be explained by close proximity of the measurement site to an avenue. Both the number and fraction of EC-containing particles in clean period was higher than NYE and GOW, in agreement with the previous conclusion that firework displays had less influence on EC compared with other urban sources (Cheng et al., 2014). Although no distinct spikes were found, fireworks-related clusters accounted for 14.8% of SPAMS analyzed particles in clean period. Episodic firework displays commonly happen during the entire spring festival holidays, so fireworks-related clusters also increased a little during nighttime.

2.4. Secondary aerosol formation

Higher than average mass ratios of SO_4^{2-}/NO_3^- have been frequently obtained in the course of firework displays (Drewnick et al., 2006; Feng et al., 2012; Pachauri et al., 2013;

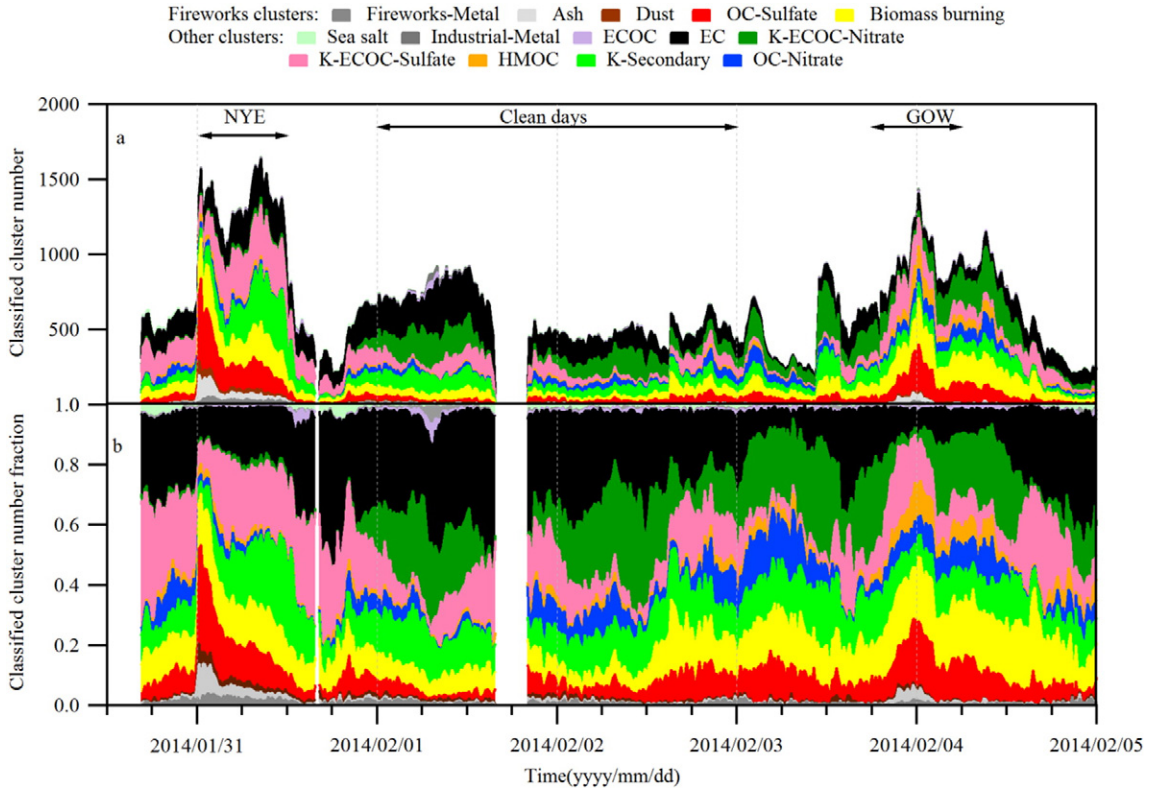

Fig. 5 – Temporal variations of different cluster counts (a) and particle number fraction (b) with 15-min time resolution.

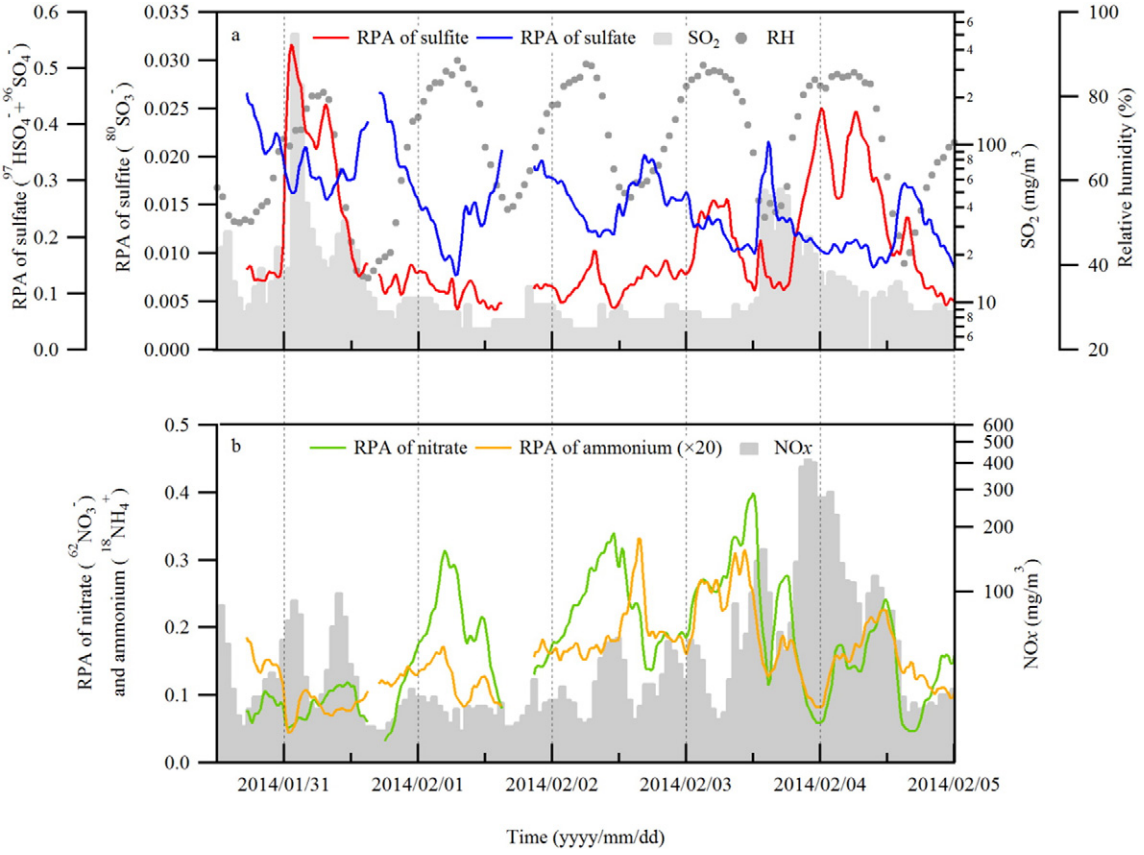

Fig. 6 – Variations of the average relative areas (RPA) of sulfite ($80SO_3^-$) and sulfate ($97HSO_4^- + 96SO_4^-$) (a) and nitrate (NO_3^- and ammonium (NH_4^+) (b).

Tian et al., 2014), emphasizing the facilitation of sulfate formation. Although SPAMS is unable to provide quantitative results due to matrix effect, relative intensities of inorganic specific ions can be used to qualitatively represent chemical composition variations on particles (Gross et al., 2000) .

2.4.1. Sulfate

Fig. 6a shows the temporal profiles of the average relative intensities of sulfate ($97HSO_4^-$+$96SO_4^-$) and sulfite ($80SO_3^-$) in individual particles. Peak of *m/z* $80SO_3^-$ is commonly recognized as a fragment ion generated from sulfates (Denkenberger et al., 2007; Moffet et al., 2008). However, the different fragment ion ratios in the reference mass spectra of Na_2SO_3 and Na_2SO_4 particles suggest that the relative intensity of $80SO_3^-$ with respect to the sum of the relative intensities of $97HSO_4^-$ and $96SO_4^-$ can be used to detect the presence of sulfites in particles. More detailed explanations can be found in supplementary information section and in Fig. S4. As shown in Fig. 6a, $80SO_3^-$ exhibited high relative intensity around midnight of NYE and GOW, while relative intensity of sulfate ($97HSO_4^-$ + $96SO_4^-$) decreased, confirming the increase of sulfite in particle phase during firework displays. The particulate sulfite increased along with the increase of SO_2 under high RH (>75%) condition during NYE, suggesting the aqueous uptake of SO_2 took place. It should be noted that the relative intensity of sulfite ($80SO_3^-$) also increased around 31-Jan-2014 3:00 and on GOW along with increasing RH and particle loadings under low SO_2 concentration. The increase of particle number and environmental humidity resulted in more aqueous surfaces which might promote the uptake of SO_2 even under low gaseous SO_2 condition. After dissolution of gaseous SO_2 in aerosol water or cloud droplets, sulfites can be oxidized into sulfates by H_2O_2, O_3,

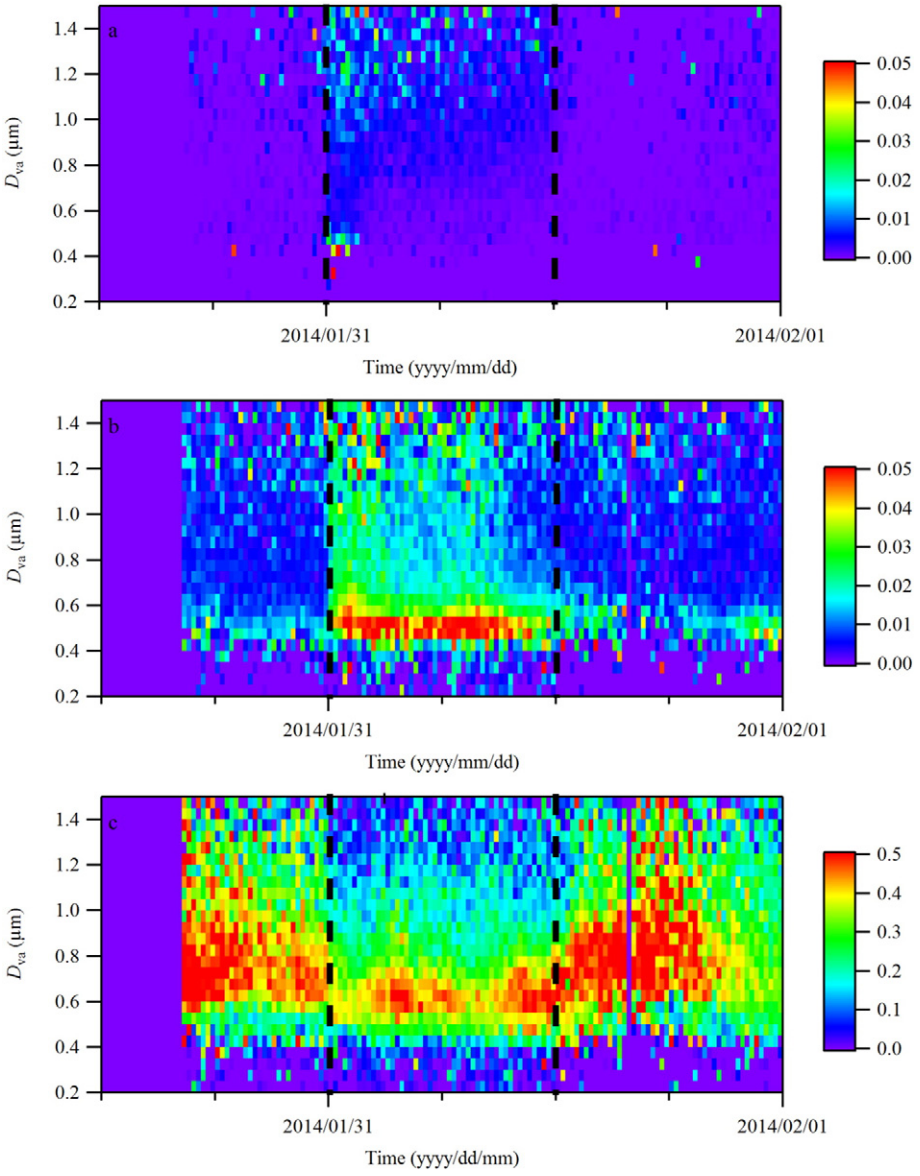

Fig. 7 – Average relative areas of $113KCl^+$ (a), sulfite ($80SO_3^-$) (b) and sulfate ($97HSO_4^-$ + $96SO_4^-$) (c) varied with particle vacuum aerodynamic diameter diameters (D_{va}) detected by single particle mass spectrometer (SPAMS) during NYE event. The dashed black lines mark the beginning and ending of New Year's Eve (NYE) pollution period.

O_2 (metal catalyzed), organic peroxides or OH radicals (Rattigan et al., 2000; Seinfeld and Pandis, 2006). Indeed, the relative intensity of sulfate ($97HSO_4^-$ + $96SO_4^-$) gradually increased after the increase of sulfite ($80SO_3^-$) and exhibited prominent values after NYE and GOW, confirming the occurrence of aqueous oxidation of sulfur in particle phase.

Additionally, Fig. 7 displays average single particle relative intensities of $113KCl^+$, $80SO_3^-$ and sulfate ($97HSO_4^-$ + $96SO_4^-$) varied among particles with different diameters. $113KCl^+$ and part of $80SO_3^-$ exhibited high intensities in particles larger than 0.9 μm, representing the residues of black powder (ash particles): KCl and K_2SO_4/K_2SO_3. Meanwhile, $80SO_3^-$ and sulfate ($97HSO_4^-$ + $96SO_4^-$) had higher intensities on smaller particles less than 0.7 μm. The different diameter distributions suggest that sulfate and sulfite compounds were mainly generated from secondary processes and direct emissions played a less significant role. Moreover, the particle diameter for which ($97HSO_4^-$ + $96SO_4^-$) had the highest intensity was around 620 nm, which was at least 50 nm larger than the particle diameter in which $80SO_3^-$ had the highest intensity. The difference suggests sulfate ($97HSO_4^-$+$96SO_4^-$) might be a reaction product of sulfite ($80SO_3^-$), with the particle size increasing during particle aging process.

In summary, our observations suggest that aqueous oxidation played a significant role in secondary sulfate formation during firework displays. Similar conclusions were reached into previous observations of the Lantern Festival in Shanghai (Wang et al., 2007). However, several researchers drew opposite conclusions that aqueous-phase oxidation of SO_2 was minor in importance relative to the direct emissions of sulfate during CNY (Feng et al., 2012; Jiang et al., 2015). The different results among these studies may be due to the special weather condition of Nanning city during wintertime, which was warmer and more humid, providing feasible prerequisites for aqueous reaction pathway.

2.4.2. Nitrate

Fig. 6b shows the temporal profile of the average relative intensity of nitrate ($62NO_3^-$) in individual particles, compared with the NOx concentration. The variation of the NOx concentration confirmed that firework displays are emission sources of NOx. However, nitrate exhibited lower relative intensity on NYE and GOW events compared with other sampling periods. Although the strong sulfate signal could suppress the relative intensity of nitrate signal, this observation indicated that firework displays had a minor impact on the formation of particulate nitrate compared to sulfate. Similar results were also observed by quantitative observations during CNY (Drewnick et al., 2006; Feng et al., 2012; Yang et al., 2014).

As shown in Fig. 6b, the intensity of nitrate gradually increased after firework detonations during NYE and GOW. NOx concentration was anti-correlated with O_3 during NYE ($r = -0.75$) and GOW ($r = -0.63$), suggesting that NOx might be oxidized to HNO_3 in gas phase. The heterogeneous formation of NH_4NO_3 on particle phase was only observed during GOW, with significant correlation ($r = 0.92$) between ammonium and nitrate observed between 3-Feb-2014 and 5-Feb-2014 by SPAMS. After the NYE, pollutants emitted from firework displays were quickly purged by clean air masses from the sea, so the condensation of NH_4NO_3 was likely suppressed. However, in the case of GOW, low wind speed and week vertical mixing were beneficial to the accumulation of gaseous precursors NH_3 and NOx, promoting the condensation of NH_4NO_3 on particles. It should be noted that severe firework displays usually occurred during winter-time in China when atmospheric thermal inversion commonly happened. So the secondary formation of nitrate caused by firework displays could be part of the reasons for the air pollution during CNY.

3. Conclusions

We investigated the evolution of the chemical composition of aerosols during traditional Chinese New Year with time-resolved single particle mass spectrometry measurements. Fireworks made an obvious contribution to accumulation mode (100–500 nm) particle number, $PM_{2.5}$ and SO_2 mass concentration. Via chemical classification of single particle, five clusters closely related to firework displays were identified: Fireworks-metal, ash, dust, OC-sulfate and biomass burning particles. Firework-related particles contributed to 70% and 50% of total particle in maximum in two separate firework pollution events (CNY and GOW).

The formation of secondary particulate sulfate and nitrate was also investigated on single particles. By distinguishing sulfite and sulfate, the result convinced the aqueous phase oxidation of dissolved sulfite to be dominant mechanism of transformation of SO_2 to sulfate. The concentration of SO_2, high relative humidity and high particle loading were the most crucial factors to promote this process. Although firework displays had a minor impact on particulate nitrate formation, it was discovered that NOx emitted from firework displays could transform to nitrate via homogeneous gas oxidation and partition to particle phase through NH_4NO_3 condensation. Our study shows that under worm, humid conditions, both primary and secondary aerosols contribute to the particulate air pollution during firework displays.

Acknowledgments

This work was supported by the National Natural Science Foundation of China (Nos. 91544224, 41275126), the Ministry of Science & Technology of China (No. 2012YQ220113-4), the Ministry of Environmental Protection of China (No. 201409008), and the Science & Technology Commission of Shanghai Municipality (No. 14DZ1202900).

Appendix A. Supplementary data

Supplementary data to this article can be found online at http://dx.doi.org/10.1016/j.jes.2016.04.021.

REFERENCES

Barman, S.C., Singh, R., Negi, M.P.S., Bhargava, S.K., 2008. Ambient air quality of Lucknow City (India) during use of fireworks on Diwali festival. Environ. Monit. Assess. 137 (1–3), 495–504.

Beig, G., Chate, D.M., Ghude, S.D., Ali, K., Satpute, T., Sahu, S.K., et al., 2013. Evaluating population exposure to environmental pollutants during Deepavali fireworks displays using air quality measurements of the SAFAR network. Chemosphere 92 (1), 116–124.

Camilleri, R., Vella, A.J., 2010. Effect of fireworks on ambient air quality in Malta. Atmos. Environ. 44 (35), 4521–4527.

Cheng, Y., Engling, G., He, K.B., Duan, F.K., Du, Z.Y., Ma, Y.L., et al., 2014. The characteristics of Beijing aerosol during two distinct episodes: impacts of biomass burning and fireworks. Environ. Pollut. 185, 149–157.

Crespo, J., Yubero, E., Nicolas, J.F., Lucarelli, F., Nava, S., Chiari, M., et al., 2012. High-time resolution and size-segregated elemental composition in high-intensity pyrotechnic exposures. J. Hazard. Mater. 241, 82–91.

Croteau, G., Dills, R., Beaudreau, M., Davis, M., 2010. Emission factors and exposures from ground-level pyrotechnics. Atmos. Environ. 44 (27), 3295–3303.

Dall'Osto, M., Harrison, R.M., 2006. Chemical characterisation of single airborne particles in Athens (Greece) by ATOFMS. Atmos. Environ. 40 (39), 7614–7631.

Denkenberger, K.A., Moffet, R.C., Holecek, J.C., Rebotier, T.P., Prather, K.A., 2007. Real-time, single-particle measurements of oligomers in aged ambient aerosol particles. Environ. Sci. Technol. 41 (15), 5439–5446.

Do, T.M., Wang, C.F., Hsieh, Y.K., Hsieh, H.F., 2012. Metals present in ambient air before and after a Firework Festival in Yanshui, Tainan, Taiwan. Aerosol Air Qual. Res. 12 (5), 981–993.

Drewnick, F., Hings, S.S., Curtius, J., Eerdekens, G., Williams, J., 2006. Measurement of fine particulate and gas-phase species during the New Year's fireworks 2005 in Mainz, Germany. Atmos. Environ. 40 (23), 4316–4327.

Dutschke, A., Lohrer, C., Kurth, L., Seeger, S., Barthel, M., Panne, U., 2011. Aerosol emissions from outdoor firework displays. Chem. Eng. Technol. 34 (12), 2044–2050.

Feng, J.L., Sun, P., Hu, X.L., Zhao, W., Wu, M.H., Fu, J.M., 2012. The chemical composition and sources of $PM_{2.5}$ during the 2009 Chinese New Year's holiday in Shanghai. Atmos. Res. 118, 435–444.

Gross, D.S., Galli, M.E., Silva, P.J., Prather, K.A., 2000. Relative sensitivity factors for alkali metal and ammonium cations in single particle aerosol time-of-flight mass spectra. Anal. Chem. 72 (2), 416–422.

Guo, S., Hu, M., Zamora, M.L., Peng, J.F., Shang, D.J., Zheng, J., et al., 2014. Elucidating severe urban haze formation in China. PNAS 111 (49), 17373–17378.

Huang, K., Zhuang, G.S., Lin, Y., Wang, Q., Fu, J.S., Zhang, R., et al., 2012. Impact of anthropogenic emission on air quality over a megacity — revealed from an intensive atmospheric campaign during the Chinese Spring Festival. Atmos. Chem. Phys. 12 (23), 11631–11645.

Jeong, C.H., McGuire, M.L., Godri, K.J., Slowik, J.G., Rehbein, P.J.G., Evans, G.J., 2011. Quantification of aerosol chemical composition using continuous single particle measurements. Atmos. Chem. Phys. 11 (14), 7027–7044.

Jiang, Q., Sun, Y.L., Wang, Z., Yin, Y., 2015. Aerosol composition and sources during the Chinese Spring Festival: fireworks, secondary aerosol, and holiday effects. Atmos. Chem. Phys. 15 (11), 6023–6034.

Kong, S., Li, L., Li, X., Yin, Y., Chen, K., Liu, D., et al., 2014. The impacts of fireworks burning at Chinese Spring Festival on air quality and human health: insights of tracers, source evolution and aging processes. Atmos. Chem. Phys. Discuss. 14 (21), 28609–28655.

Kong, S.F., Li, X.X., Li, L., Yin, Y., Chen, K., Yuan, L., et al., 2015a. Variation of polycyclic aromatic hydrocarbons in atmospheric $PM_{2.5}$ during winter haze period around 2014 Chinese Spring Festival at Nanjing: insights of source changes, air mass direction and firework particle injection. Sci. Total Environ. 520, 59–72.

Kong, S.F., Li, L., Li, X.X., Yin, Y., Chen, K., Liu, D.T., et al., 2015b. The impacts of firework burning at the Chinese Spring Festival on air quality: insights of tracers, source evolution and aging processes. Atmos. Chem. Phys. 15 (4), 2167–2184.

Lemieux, P.M., Lutes, C.C., Santoianni, D.A., 2004. Emissions of organic air toxics from open burning: a comprehensive review. Prog. Energy Combust. Sci. 30 (1), 1–32.

Li, L., Huang, Z.X., Dong, J.G., Li, M., Gao, W., Nian, H.Q., et al., 2011. Real time bipolar time-of-flight mass spectrometer for analyzing single aerosol particles. Int. J. Mass Spectrom. 303 (2–3), 118–124.

Li, W., Shi, Z., Yan, C., Yang, L., Dong, C., Wang, W., 2013. Individual metal-bearing particles in a regional haze caused by firecracker and firework emissions. Sci. Total Environ. 443, 464–469.

Li, L., Li, M., Huang, Z.X., Gao, W., Nian, H.Q., Fu, Z., et al., 2014. Ambient particle characterization by single particle aerosol mass spectrometry in an urban area of Beijing. Atmos. Environ. 94, 323–331.

Liu, D.Y., Rutherford, D., Kinsey, M., Prather, K.A., 1997. Real-time monitoring of pyrotechnically derived aerosol particles in the troposphere. Anal. Chem. 69 (10), 1808–1814.

McGuire, M.L., Jeong, C.H., Slowik, J.G., Chang, R.Y.W., Corbin, J.C., Lu, G., et al., 2011. Elucidating determinants of aerosol composition through particle-type-based receptor modeling. Atmos. Chem. Phys. 11 (15), 8133–8155.

Moffet, R.C., de Foy, B., Molina, L.T., Molina, M.J., Prather, K.A., 2008. Measurement of ambient aerosols in northern Mexico City by single particle mass spectrometry. Atmos. Chem. Phys. 8 (16), 4499–4516.

Moreno, T., Querol, X., Alastuey, A., Minguillon, M.C., Pey, J., Rodriguez, S., et al., 2007. Recreational atmospheric pollution episodes: inhalable metalliferous particles from firework displays. Atmos. Environ. 41 (5), 913–922.

Nishanth, T., Praseed, K.M., Rathnakaran, K., Satheesh Kumar, M.K., Ravi Krishna, R., Valsaraj, K.T., 2012. Atmospheric pollution in a semi-urban, coastal region in India following festival seasons. Atmos. Environ. 47 (0), 295–306.

Pachauri, T., Singla, V., Satsangi, A., Lakhani, A., Kumari, K.M., 2013. Characterization of major pollution events (dust, haze, and two festival events) at Agra, India. Environ. Sci. Pollut. Res. 20 (8), 5737–5752.

Puri, V., Mahendru, S., Rana, R., Deshpande, M., 2009. Firework injuries: a ten-year study. J. Plast. Reconstr. Aesthet. Surg. 62 (9), 1103–1111.

Rattigan, O.V., Boniface, J., Swartz, E., Davidovits, P., Jayne, J.T., Kolb, C.E., et al., 2000. Uptake of gas-phase SO_2 in aqueous sulfuric acid: oxidation by H_2O_2, O_3, and HONO. J. Geophys. Res. 105 (D23), 29065–29078.

Sarkar, S., Khillare, P.S., Jyethi, D.S., Hasan, A., Parween, M., 2010. Chemical speciation of respirable suspended particulate matter during a major firework festival in India. J. Hazard. Mater. 184 (1–3), 321–330.

Seinfeld, J.H., Pandis, N.S., 2006. Atmospheric Chemistry And Physics: From Air Pollution to Climate Change. second ed. John Wiley & Sons, New York.

Shi, Y.L., Zhang, N., Gao, J.M., Li, X., Cai, Y.Q., 2011. Effect of fireworks display on perchlorate in air aerosols during the Spring Festival. Atmos. Environ. 45 (6), 1323–1327.

Sijimol, M.R., Mohan, M., 2014. Environmental impacts of perchlorate with special reference to fireworks—a review. Environ. Monit. Assess. 186 (11), 7203–7210.

Silva, P.J., Prather, K.A., 2000. Interpretation of mass spectra from organic compounds in aerosol time-of-flight mass spectrometry. Anal. Chem. 72 (15), 3553–3562.

Song, X.H., Hopke, P.K., Fergenson, D.P., Prather, K.A., 1999. Classification of single particles analyzed by ATOFMS using an artificial neural network, ART-2A. Anal. Chem. 71 (4), 860–865.

Tian, Y.Z., Wang, J., Peng, X., Shi, G.L., Feng, Y.C., 2014. Estimation of the direct and indirect impacts of fireworks on the

physicochemical characteristics of atmospheric PM_{10} and $PM_{2.5}$. Atmos. Chem. Phys. 14 (18), 9469–9479.

Tsai, H.-H., Chien, L.-H., Yuan, C.-S., Lin, Y.-C., Jen, Y.-H., Ie, I.-R., 2012. Influences of fireworks on chemical characteristics of atmospheric fine and coarse particles during Taiwan's Lantern Festival. Atmos. Environ. 62 (0), 256–264.

Wang, Y., Zhuang, G.S., Xu, C., An, Z.S., 2007. The air pollution caused by the burning of fireworks during the lantern festival in Beijing. Atmos. Environ. 41 (2), 417–431.

Wang, X.N., Ye, X.N., Chen, H., Chen, J.M., Yang, X., Gross, D.S., 2014. Online hygroscopicity and chemical measurement of urban aerosol in Shanghai, China. Atmos. Environ. 95 (0), 318–326.

Yang, L.X., Gao, X.M., Wang, X.F., Nie, W., Wang, J., Gao, R., et al., 2014. Impacts of firecracker burning on aerosol chemical characteristics and human health risk levels during the Chinese New Year Celebration in Jinan, China. Sci. Total Environ. 476, 57–64.

Yerramsetti, V.S., Sharma, A.R., Navlur, N.G., Rapolu, V., Dhulipala, N., Sinha, P.R., 2013. The impact assessment of Diwali fireworks emissions on the air quality of a tropical urban site, Hyderabad, India, during three consecutive years. Environ. Monit. Assess. 185 (9), 7309–7325.

Zhang, M., Wang, X.M., Chen, J.M., Cheng, T.T., Wang, T., Yang, X., et al., 2010. Physical characterization of aerosol particles during the Chinese New Year's firework events. Atmos. Environ. 44 (39), 5191–5198.

Zhao, S.P., Yu, Y., Yin, D.Y., Liu, N., He, J.J., 2014. Ambient particulate pollution during Chinese Spring Festival in urban Lanzhou, Northwestern China. Atmos. Pollut. Res. 5 (2), 335–343.